REQUIREMENTS FOR OBSERVATION SCENARIOS TO MAINTAIN A CATALOGUE OF SPACE DEBRIS OBJECTS IN GEOSYNCHRONOUS REGION

A. Hinze[(1)], H. Fiedler[(1)], and T. Schildknecht[(2)]

[(1)]*DLR, 82234 Weßling, Germany, Email: {Andreas.Hinze, Hauke.Fiedler}@dlr.de*
[(2)]*Astronomical Institute University Bern, 3012 Bern, Switzerland, Email: Thomas.Schildknecht@aiub.unibe.ch*

ABSTRACT

Optical observations for space debris in the geosynchronous region have been performed for many years. During this time, observation strategies, processing techniques and cataloguing approaches were successfully developed. The importance of protecting this orbital region from space debris requires continuous surveying and monitoring in order to support collision avoidance operations. Further observations of the objects, providing information for orbit improvement calculations, are helping to maintain high accuracy ephemeris of the catalogued objects.
This paper presents an analysis of the possibility to re-observe the objects within a catalogue by taking into account the orbit accuracy represented by their covariance matrix. Estimating process noise and measurement noise covariances, Kalman filtering is applied to assess the frequency and the number of necessary follow-up observations for catalogue maintenance. For reliable re-observations of the objects, observation constraints like e.g. the field of view are taken into account. Finally orbits of selected objects are determined and propagated to validate the results.

1. INTRODUCTION

The space debris population around the Earth is permanently increasing. Objects in lower altitudes like in the Low Earth Orbit (LEO) are monitored by radar telescopes which are less dependent on weather and time conditions. Optical observations are used to observe space debris objects in higher altitudes. One of the most important and valuable orbit around the Earth is the Geosynchronous Earth Orbit (GEO). During the last years, several survey strategies have been developed to build up a catalogue of space debris objects for characterizing, collision avoidance and to improve the knowledge of the population size. If once a determined orbit of a GEO object is good enough to re-observe this object after several days this orbit may be added to the catalogue. Simulations showed that after four observation sequences such a secure orbit may be determined [4]. Anyway, for catalogue maintenance, additional observations are necessary to improve the orbit and to keep the orbit accuracy within a given limit. Since the GEO has to be observed with optical telescopes, the length of the observation night, which depends on the location site of the telescope and the season, is the most limiting factor. Depending on the used telescope and its Field of View (FoV), the position inaccuracy should be less than the half FoV to ensure a successful re-detection. Scheduling follow-up observations (FuP) for catalogued space debris objects requires an accurate propagation of the estimated state and the related error ensuring an optimized use of the observation resources. During the propagation systematic errors caused by small non-linearities, round-off errors or simplifications of the force and measurement model arises. On way to deal with that is to add a small noise term with each propagation time step to avoid that the covariance matrix diverge after a certain amount of measurements.

2. ANALYSIS OF CATALOGUED OBJECTS

Since a long time the Astronomical Institute University Bern (AIUB) observes space debris in several orbital regions for the scientific purpose. The focus of these observations is to find objects with high area-to-mass ratios (AMR) [6]. In addition to the own 1-m ZIMLAT telescope and the robotic experimental ZimSMART telescope in Zimmerwald, Switzerland, observations were performed with the ESA Space Debris Telescope (ESASDT) at the Optical Ground Station (OGS), Observatorio del Teide, Tenerife. All discovered objects were catalogued and follow-up observations were performed for catalogue maintenance where each telescopes mostly maintains his own catalogue. At ESASDT monthly observation campaigns of few nights around to the new moon phase were used for space debris observations. Since there is no optimized scheduling algorithm, objects were selected by the observer according to their visibility, AMR, orbital parameters and the time since the last successful observation. Observations with ZIMLAT were scheduled with a simple scheduling algorithm based on priorities classes of the objects. Each object was classified according to the visibility, time since the last observation, AMR and the phase angle during the night. Fi-

nally ZimSMART performed only surveys in high density regions [2]. It has to be noted, that both telescopes in Zimmerwald are not only used for space debris observations what reduces the available observation time, too.
Nevertheless, over the time objects had to be excluded from the active observation catalogue since they could not be observed for a longer time. There are a plenty of reasons for such a lack of observations. One general reason is the changing visibility of the objects over the time. Further faint objects might not be detected because of the limited sensitivity by the sensor and a not optimized phase angle observation. But also the orbital elements themselves and their evolution affect the performance of the observations. With a limited distribution of available telescopes only a short part of the orbit can be observed. Therefore the accuracy for the non-observed part is poor. This effect increases with higher eccentricities and AMR values and affect therefore the frequency of necessary follow-up observations significantly. Finally the quality of the determined orbit and the related accuracy terminate the time span to the next follow-up observation. Depending on the FoV of the used telescope this time span can vary.
During the last 15 years AIUB discovered with these three telescopes about 2500 objects in GEO. About 950 objects could be observed in the subsequent nights and elliptical orbits have been determined. Finally about 410 objects were observed longer than three months. Figure 1 shows the final arc length with observations for these objects versus the time since the last observation epoch. Most of the objects with eccentricities higher than 0.02 (blue and red) have been observed for one or two years. At this time almost all objects were observed with ESASDT during the monthly observation campaigns. Note, that the ESASDT has only a FoV of $0.7°$x $0.7°$ and an orbit with poor accuracy results in an high position inaccuracy which reduces the probability of successful FuP after several weeks. Further, because of bad weather condition or other reasons some observations campaigns could not be performed and therefore the time between the observations campaigns might increased up to few weeks. Anyway, this result is a first hint that these kind of objects should be observed more than once per month. As mentioned above, the focus of the observation campaigns was to detect and catalogue objects with high AMR values. Figure 2 shows the AMR values versus the time since the last observation and Figure 3 shows the eccentricity versus the time since the last observation for the selected 410 objects. The distribution of the objects can be explained by the fact, that orbits in GEO are strongly influenced by the solar radiation pressure what leads to high eccentricities for objects with high AMR values.

Finally the orbit accuracy determines the frequency of necessary FuP observations for catalogue maintenance. A poor accuracy in the semi-major axis leads to a poor estimation of the velocity and reduces therefore the probability of a successful FuP after a certain time. Figure 4 shows the error in the semi major axis after the last orbit determination versus the time since the last observation. Objects with higher eccentricities have a slightly higher mean value of about 55 m whereas objects with lower eccentricities have a mean value of about 44 m. Neverthe-

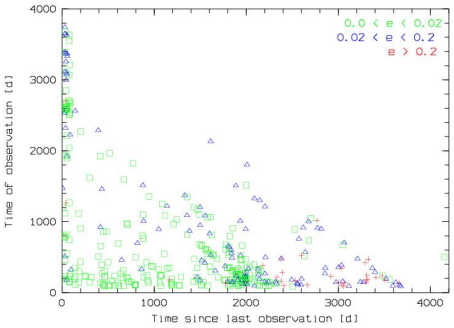

Figure 1. Final arc length vs. time since the last observation for 410 objects observed longer than 90 nights. Object in green have an eccentricity of less than 0.02, blue between 0.02 and 0.2 and red higher than 0.2.

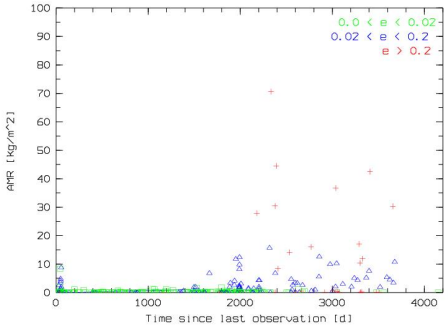

Figure 2. Estimated AMR value vs. time since the last observation for 410 objects observed longer than 90 nights. Object in green have an eccentricity of less than 0.02, blue between 0.02 and 0.2 and red higher than 0.2.

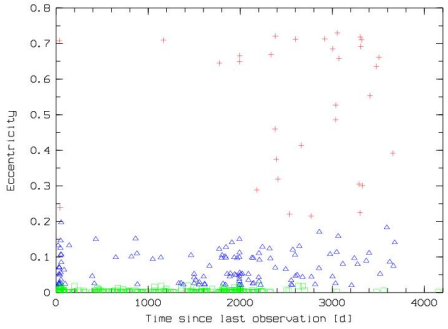

Figure 3. Estimated eccentricity vs. time since the last observation for 410 objects observed longer than 90 nights. Object in green have an eccentricity of less than 0.02, blue between 0.02 and 0.2 and red higher than 0.2.

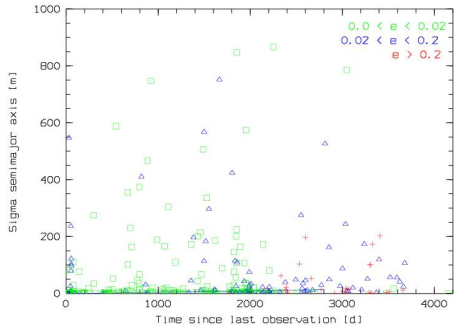

Figure 4. The error of the semi-major axis after the last orbit determination versus the time since the last observation for 410 objects observed longer than 90 nights. Object in green have an eccentricity of less than 0.02, blue between 0.02 and 0.2 and red higher than 0.2.

less, more than 80 % of the objects have an accuracy of better than 50 m. The orbit accuracy depends on the one hand from the accuracy of the observations and on the other hand of the number of used observation during the orbit determination process. The rms value of the residuals can be used as a quantitation of the determined orbit and was empirical limited to $2''$. If this value was exceeded the used observation arc was reduced and the orbit was determined again until the rms value was below the given limit. Since all catalogued objects were observed with the same telescopes the measurement accuracy is comparable and not considered in detail. Depending on the orbital elements and the AMR values it is expected that different arc lengths are used for the orbit determination. Table 1 shows the estimated semi-major axis, eccentricity, AMR value, the magnitude and the error of the semi-major axis after the last orbit determination of some selected objects. All objects were observed in total longer than 90 days and their orbits allow a re-observation after a certain time. Figure 5 shows the length used for the orbit determination versus the total available arc length for the selected objects. For objects with a very low eccentricity arc length of up to 300 nights can be used for an orbit determination within the given limits. Whereas with increasing eccentricity and AMR value the used arc length decreases up to about 50 nights. Latter requires observation more than once per month to ensure a successful FuP observation in the future and to keep the object in the catalogue. Nearly circular orbits require less observations and once per two or three months should be sufficient for catalogue maintenance.

3. METHOD

The mathematical description of the covariance matrix is shown e.g. in [7], [3]. Usually the notation uses P and the covariance matrix is given by:

$$P = (A^T W A)^{-1} \tag{1}$$

Table 1. Chosen values for some selected objects.

Name	Axis [km]	ecc	AMR	mag	σ_a [m]
E06293A	40277.3	0.22	16.1	16.2	13.3
E06349B	41891.5	0.005	0.42	17.1	0.88
E07014A	42145.2	0.31	17.1	00.0	4.07
E07337C	42427.1	0.044	1.95	16.9	4.58
S90009	42276.5	0.003	0.005	16.4	0.64
Z11101I	42166.8	0.001	0.01	12.6	1.11

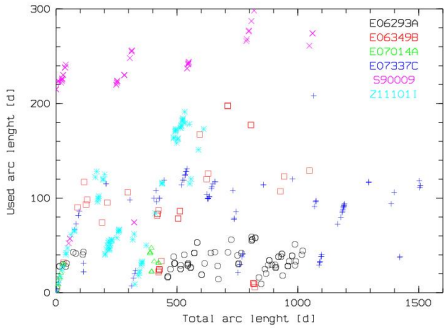

Figure 5. Used arc length for orbit determination vs. total available arc length for some selected objects.

where A is the partial-derivative matrix (partial derivatives of the observations with respect to the estimated parameters), and W the measurement noise matrix. The correct computation of P requires a good a priori knowledge of the measurement standard deviation represented by the matrix W. Next to this, the covariance depends only on the partial-derivative matrix A and therefore only on the type and distribution of the measurements. Any changes of the state vector at a specified epoch t_0 to another epoch t are described by the state transition matrix Φ. A time update of the covariance matrix is than given by:

$$\bar{P}_{t+1} = \Phi \bar{P}_{t_0} \Phi^T + Q \tag{2}$$

where Q is the process noise matrix. Adding small noise terms with each time update seems to be necessary since the determined covariance matrix often found to be too optimistic in the presence of systematic force and measurement model errors [3]. Using sequential estimation e.g. Kalman filter for the orbit determination, after a certain amount of measurements the covariance matrix and the Kalman gain diverge to zero what inhibit further improvements. The measurement update of the Kalman filter is given by:

$$\hat{P}_{t+1} = \bar{P}_{t+1} - K_{t+1} H \bar{P}_{t+1} \tag{3}$$

with H as the measurement-state partial matrix and K as the Kalman gain.
The difficulty is to specify Q without a priori knowledge. One approach to approximate the process noise matrix

is to use the uncertainty of parameters within the acceleration model. To validate these results Precision Orbit Ephemeris of GPS satellites can be used. Another common method to determine Q is by trail and error and to see how does it works. Since we are interested in the estimation of the time to the next follow-up observations, different values of the process noise are assumed and the results are compared with the analysis of Section 2. Adding a constant process noise matrix with each time update is sufficient since a constant step size is applied.
For the orbit determination process real observations of selected objects were used. The perturbation due to the gravitational attractions by the Sun and Moon, the Earth's potential coefficients up to terms of degree and order 12, and the direct radiation pressure are taken into account for all computations.

4. CASE STUDIES

The following case studies are based on real observations performed during the last years by several telescopes e.g. ESASDT, ZIMLAT. This approach is used to analyse on real observation conditions. Usually all observations of the same object within a single FoV crossing constitute a so-called tracklet. A tracklet is a set of observations acquired over short period of time which presumably belong to the same object. Such tracklets have been performed by the telescopes and they are distributed randomly according to the observations conditions at given time and station.
At first, different values for the process noise were analysed according to the influence of the orbit determination process depending on the object characteristics. Finally three different cases were specified and are summarised in Table 2. A standard deviation of $1''$ is chosen for the measurement noise. For the initial state a priori standard deviation twice worse than the expected values after the orbit determination is assumed ensuring that the filter starts properly. In the first case A no process noise is added. The second case B is optimized according to objects in GEO with low eccentricity. Figure 6 shows the filter performance for an observations arc of about 100 days including a longer period of no observations. The correction of the state by the Kalman gain is minimized in comparison with other process noise values also after a longer time of no observations. The measurement errors (errors in azimuth seen from ZIMLAT in Zimmerwald/Switzerland) are shown in Figure 7. Case B confirms with the assumptions in [1] and [5]. Finally the third case C is optimized for objects with high area-to-mass ratios (HAMR) and the results are shown in Figure 8.

From the AIUB space debris catalogue objects which have been observed more than 10 times and with a final arc length of more than 90 days were selected. These limits were chossen ensuring well estimated orbital values. The previous analysis showed that depending on the orbital elements and the specifications of the object different observation strategies are required. Therefore the selected objects were divided in three groups according to their previous estimated AMR values and the eccentricity

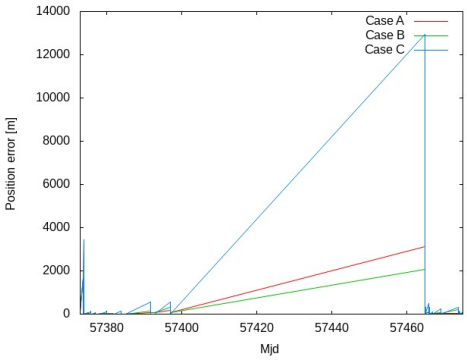

Figure 6. Position error performing sequential orbit determination of object E10012B with low eccentricity. Each colour represents a different noise matrix: red (Case A), green (Case B) and blue (Case C).

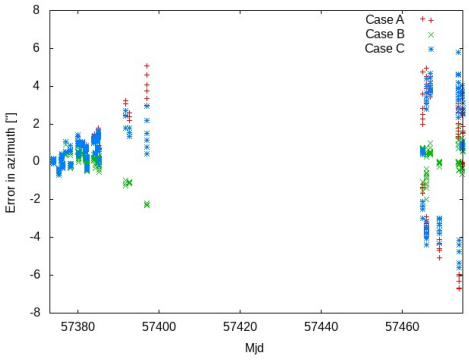

Figure 7. Measurement error in azimuth (seen from Zimmerwald/Switzerland) performing sequential orbit determination of object E10012B with low eccentricity. Each colour represents a different noise matrix: red (Case A), green (Case B) and blue (Case C).

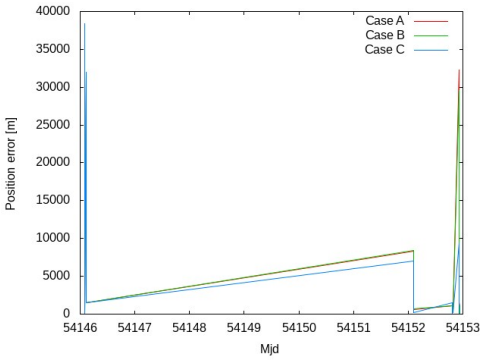

Figure 8. Position error performing sequential orbit determination of object E06204D with high eccentricity. Each colour represents a different noise matrix: red (Case A), green (Case B) and blue (Case C).

Table 2. Filter parameters for selected case studies

Parameter		Case A	Case B	Case C
Measur. std. dev.	[″]	1	1	1
Position std. dev.	[m]	500.0	500.0	500.0
Velosity std. dev.	[m s^{-1}]	0.2	0.2	0.2
State noise pos.	[m]	0.0	0.03	0.03
State noise vel.	[m s^{-1}]	0.0	1.0e-7	1.0e-4

after the last orbital determination. Three objects of each group are analysed in the following section. After the orbit determination the orbit was propagated over 90 nights to illustrate the evolution of the estimated errors. Evaluating the required observation strategy, an upper limit for the error in along-track direction of $20km$ is chosen. This values is reasonable since at the altitude of GEO the value can be assumed to be linear.

4.1. Objects with low eccentricity

Objects with very low eccentricity have usually also low AMR values and the perturbation of the solar radiation pressure is limited. The orbital elements and the estimated AMR values of three selected objects are given in Table 3. In Figure 9 the evolution for the estimated errors without any added process noise are shown. After the orbit determination the estimated error in along-track is about $50m$ for all objects whereas the error in semi-major axis is between $1-2m$. After 90 days the error in along-track increased up to about $2km$ what corresponds to an angle error up to $10''$ in azimuth and elevation.
Since case B is optimized for this kind of objects, the results in Figure 10 might to be close to the reality. In comparison with case A the along-tack error after the orbit determination increased up to $100m$ and the error evolution of the objects E06349B and E10012B are now similar. After 90 days an error of about $10''$ in azimuth and elevation allows still a successful re-observations after several months. This confirms with the experience that objects with almost circular orbits have been re-observed after several months also with telescopes with a small FoV like $0.7°$x $0.7°$. Therefore no forced FuP observations strategy might be required.
Finally the results of case C are shown in Figure 11. The error in along-track is increased up to $65km$ after 90 days what corresponds to an error in azimuth and elevation of about $400''$.

Table 3. Object parameters for selected GEO objects with low eccentricity.

Orbital Elements		E06349B	E10012B	E10041A
a	[km]	41889.5	42490.9	41784.1
e		0.004	0.001	0.002
i	[°]	14.1	12.6	14.4
Ω	[°]	3.7	35.1	14.6
ω	[°]	106.5	285.0	339.0
M	[°]	55.2	199.6	241.4
AMR	[kg m^{-2}]	0.08	0.018	0.013

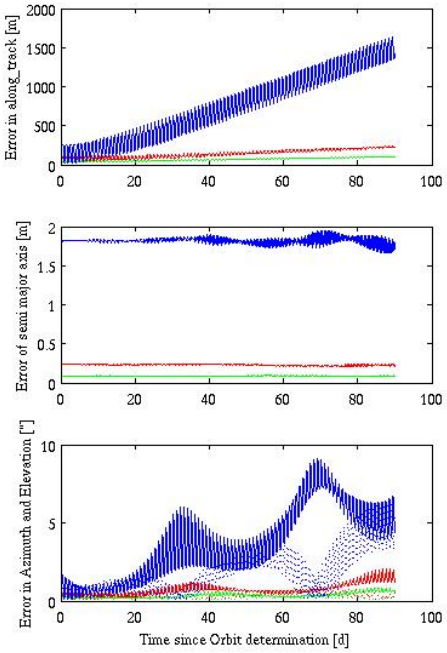

Figure 9. Case A: Error in along-track (above), semi-major axis (middle), Azimuth (bottom, solid line) and Elevation (bottom, dotted line) for the objects E06349B (red), E10012B (green) and E10041A (blue) propagated over 90 orbits.

4.2. Object with higher eccentricity

Objects with eccentricity higher 0.02 might have also a higher AMR values and the perturbation caused by the solar radiation pressure increases. Radiation pressure perturbations directly depends on the current area and its orientation to the radiation source. Since it is hard to model the proper motion of each object frequent observations are required. As mentioned above the main focus of the performed space debris observations were to detect object with high AMR values. In the following section objects with higher eccentricity and higher estimated AMR values are analysed (Table 4). To compare the performance of the orbit determination process with the regular orbit determination performed by AIUB, the same arc length of observations was taken. In comparison with the group of objects in the previous section,

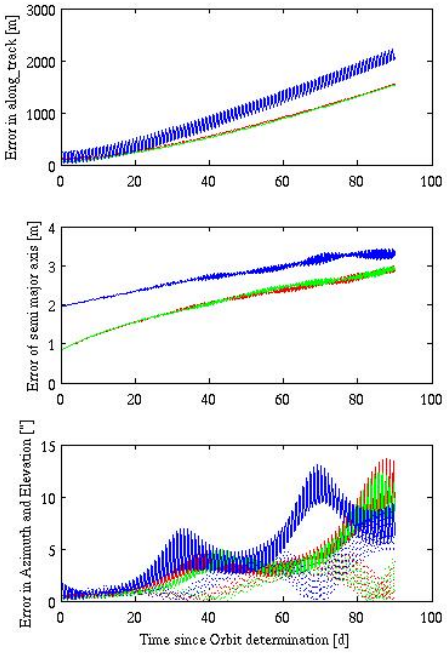

Figure 10. Case B: Error in along-track (above), semi-major axis (middle), Azimuth (bottom, solid line) and Elevation (bottom, dotted line) for the objects E06349B (red), E10012B (green) and E10041A (blue) propagated over 90 orbits.

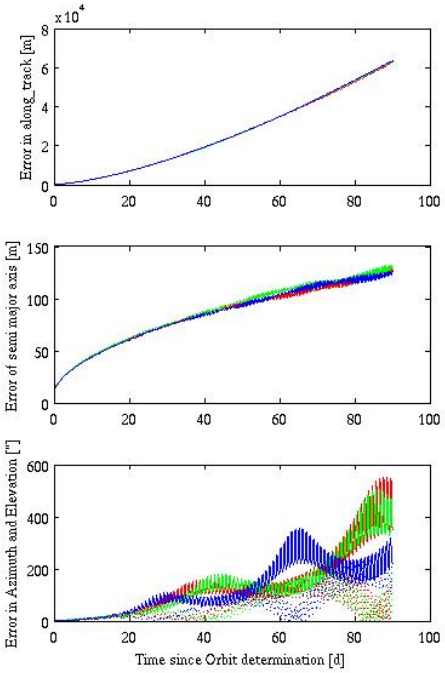

Figure 11. Case C: Error in along-track (above), semi-major axis (middle), Azimuth (bottom, solid line) and Elevation (bottom, dotted line) for the objects E06349B (red), E10012B (green) and E10041A (blue) propagated over 90 orbits.

Table 4. Object parameters for selected GEO objects with higher eccentricity.

Orbital	Elements	E07337C	E09054B	E09293A
a	[km]	42427.5	41868.6	41389.9
e		0.04	0.1	0.11
i	[°]	14.4	7.7	14.2
Ω	[°]	3.4	323.3	350.1
ω	[°]	261.7	21.6	243.8
M	[°]	130.4	28.4	176.6
AMR	[kg m^{-2}]	1.94	2.54	4.24

the errors are in general bigger caused by the increasing perturbation of the radiation pressure and by the use of less measurement points. The results of case A and B differ less as before and for case B they are shown in Figure 12. Complete different are the results after 90 days in case C (Figure 13). The error in along-track direction increased up to $80km$ and in azimuth up to $600''$. This might be still in a small FoV but in terms of object correlation and orbit accuracy the error in along-track should be less than $20km$ what requires further follow-up observation already after 20-30 days.

4.3. Objects with high elliptical orbits

Finally objects with high AMR values were analysed and the objects are summarised in Table 5. When no or just

Table 5. Object parameters for selected GEO objects with high AMR values.

Orbital	Elements	E06204D	E06207B	E08218C
a	[km]	47035.2	38556.3	36157.1
e		0.3	0.4	0.56
i	[°]	9.5	11.1	5.4
Ω	[°]	130.4	329.4	47.6
ω	[°]	309.4	282.5	161.4
M	[°]	70.9	177.7	191.2
AMR	[kg m^{-2}]	11.9	30.3	36.7

small noise is added the error in along-track increases after 90 days up to $10-15km$. In azimuth an error of about $400''-600''$ is reached. The results of case B are shown in Figure 14. But the more realistic case for this kind of objects is case C. After one month the along-track error is already up to $35km$ and the error in azimuth reaches similar values like in case A and B after 90 days. As

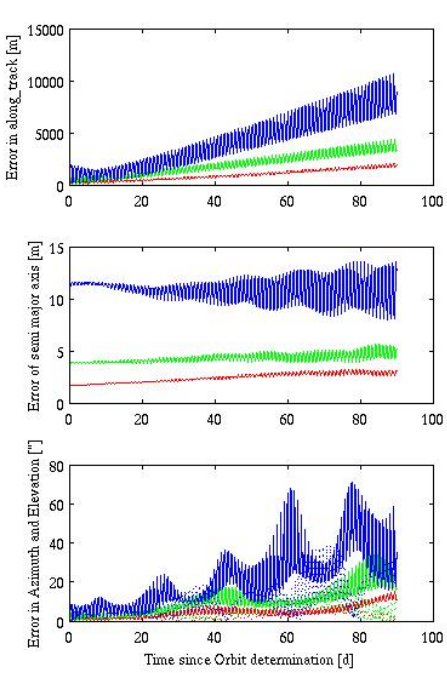

Figure 12. Case B: Error in along-track (above), semi-major axis (middle), Azimuth (bottom, solid line) and Elevation (bottom, dotted line) for the objects E07337C (red), E09054B (green) and E09293A (blue) propagated over 90 orbits.

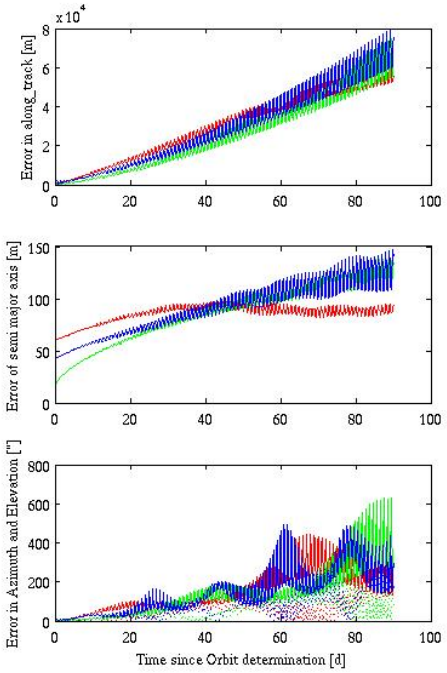

Figure 13. Case C: Error in along-track (above), semi-major axis (middle), Azimuth (bottom, solid line) and Elevation (bottom, dotted line) for the objects E07337C (red), E09054B (green) and E09293A (blue) propagated over 90 orbits.

expected the frequency of follow-up observations should be much higher for catalogue maintenance in comparison with objects is almost circular orbits. With an upper limit of $20km$ in along-track direction, these objects should be observed weekly to ensure a successful object correlation and to keep these objects in the space debris catalogue with an certain orbit accuracy.

5. CONCLUSION

In this work the space debris catalogue of AIUB was analysed to estimate the required frequency of follow-up observations for catalogue maintenance. Catalogued objects with a long observations arc were used to determine a realistic process noise matrix depending on the object characteristics. While for objects with low eccentricity and AMR value a small noise has to be added, higher values for the velocity noise are recommended for objects with higher eccentricity and AMR value. Using these results the estimated state and the related covariance matrix were propagated over 90 days and the time to the next required follow-up observations within a certain orbit accuracy was estimated. Objects with low eccentricity allow a more straightened observation strategy for catalogue maintenance in comparison with high elliptical objects, which should be observed weekly ensuring a sufficient orbit accuracy.

REFERENCES

1. V. Grigore. *Unscented Kalman Filters for Attitude and Orbit Estimation of a Low Earth Orbit CubeSat*. Master Thesis, Royal Institute of Technology, Sweden, 2015.
2. J. Herzog, T. Schildknecht, A. Hinze, M. Ploner, and A. Vananti. Space Surveillance Observations at the AIUB Zimmerwald Observatory. In *Proceedings of the 6th European Conference on Space Debris*, 2013.
3. Gill E. Montenbruck, O. *Satelittes Orbit*. Springer, 2012.
4. R. Musci, T. Schildknecht, and M. Ploner. Orbit Improvement for GEO Objects Using Follow-up Observations. *Advances in Space Research*, (34):912 – 916, 2004.
5. M. Psiaki. Satellite Orbit Determination Using a Single-Channel Global Positioning System Receiver. 2004.
6. T. Schildknecht, R. Musci, and T. Flohrer. Challenges Related to Discovery, Follow-up, and Study of Small High Area-to-Mass Ratio Objects at GEO. In *Proceedings of the AMOS Conference*, 2007.
7. D. A. Vallado. *Fundamentals of Astrodynamics and Applications*. Springer/Microcosm, Hawthorne, CA, 2007.

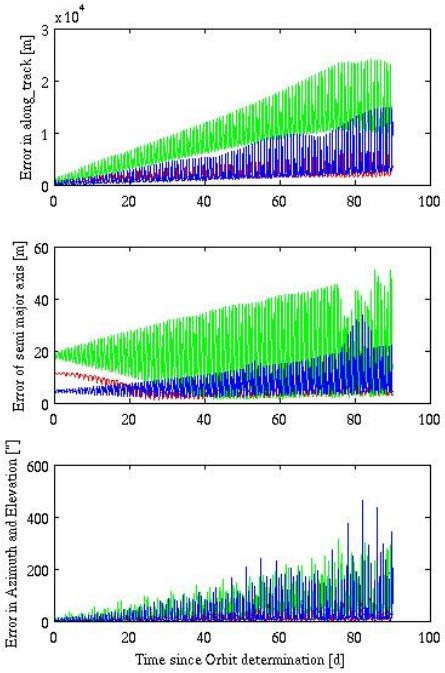

Figure 14. Case B: Error in along-track (above), semi-major axis (middle), Azimuth (bottom, solid line) and Elevation (bottom, dotted line) for the objects E06204D (red), E06207B (green) and E08218C (blue) propagated over 90 orbits.

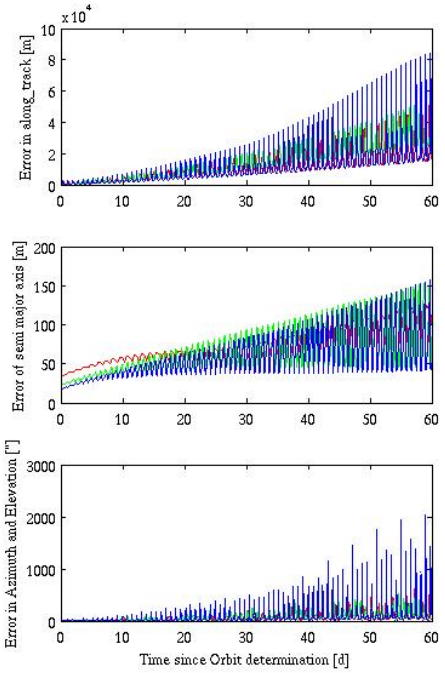

Figure 15. Case C: Error in along-track (above), semi-major axis (middle), Azimuth (bottom, solid line) and Elevation (bottom, dotted line) for the objects E06204D (red), E06207B (green) and E08218C (blue) propagated over 90 orbits.